East Asian Math. J.
Vol. 32 (2016), No. 1, pp. 129–138
http://dx.doi.org/10.7858/eamj.2016.013

THE METHOD OF REGULARIZATION RATIOS APPLIED TO RECONSTRUCTIONS OF ELASTIC RIGID OBSTACLES VIA THE FACTORIZATION METHOD

K.Kim, K.H.Leem, and G. Pelekanos

Abstract. In this paper, we propose an efficient regularization technique (The Method of Regularized Ratios) for the reconstruction of the shape of a rigid elastic scatterer from far field measurements. The approach used is based on the factorization method and creates via Picard's condition ratios, baptized Regularized Ratios, that serve to effectively remove unwanted singular values that may lead to poor reconstructions. This is achieved through the use of a sophisticated algorithm that progressively adjusts an initially set moderate tolerance. In comparison with the well established Tikhonov-Morozov regularization techniques our new algorithm appears to be more computationally efficient as it doesn't require computation of the regularization parameter for each point in the grid.

1. Introduction

It is well known that direct scattering problems have been treated by many scientists and are connected with the solution of a boundary value problem that shows how the presence of an obstacle affects the propagation of a known time-harmonic incident wave. The properties of the obstacle that enter into this scattering process are concerned with specific functions of directions far away from the obstacle which are known as scattering amplitudes or far-field patterns.

The book by Colton and Kress [6] constitutes an excellent source of information on inverse problems.

Our aim in the present paper is to extend the method of regularization ratios applied to the linear sampling method [6], initially introduced by Leem and Pelekanos [13], for the reconstruction of sound soft obstacles to the more complicated elastic scattering. In particular we will provide reconstructions of two dimensional rigid objects excited by incident elastic waves. Our method will utilize the ideas behind Kirsch's factorization method [12]. The main idea of

Received January 18, 2016; Accepted January 30, 2016.
2010 *Mathematics Subject Classification.* 15A29, 45B05, 65J22, 65F22, 65M32, 65R20, 65R30.
Key words and phrases. Regularization.

(pISSN 1226-6973, eISSN 2287-2833)

the method is that the support of the scattering obstacle is obtained by solving a vector integral equation of the first kind and noting that a specific norm becomes unbounded as a point lying on a rectangular grid containing the scatterer approaches the boundary from inside.

Kirsch's factorization method is well known to yield an ill posed far field equation customarily solved via Tikhonov regularization with the regularization constant computed via Morozov's discrepancy principle [7]. However, Morozov's discrepancy principle requires the computation of the zeros of the discrepancy function at each point of the grid, a process that is time-consuming. Moreover, the noise level in the data should be known *a priori*, something that in real life applications is not the case in general. In order to avoid these problems, the method of regularized ratios [13] will be applied to the ill posed far field equation described above and will yield faster reconstructions without a-priori knowledge of the noise level in the data. In general, the method of regularized ratios can be viewed as a systematic, efficient and sophisticated way, to eliminate useless singular values that in many cases tend to ruin the quality of the reconstructions.

We organize our paper as follows. In Section 2 we first formulate the direct scattering problem for a rigid obstacle excited by an incident elastic wave. Consequently, Section 3 will deal with the formulation of the factorization method. Finally, in Section 4 we will describe the method of regularization ratios under the framework of the factorization method and we will show its effectiveness through different reconstructions of a kite

2. Formulation of the problem

Let $D \subset \mathbb{R}^2$ denote a non penetrable obstacle which is an open, bounded and simply connected domain. The domain D has a smooth boundary ∂D of class C^2 and is embedded in a infinite isotropic and homogeneous elastic medium with Lame constants λ, μ and mass density ρ. We assume that the wave propagation elastic medium supports longitudinal as well as transverse waves; hence strong ellipticity conditions for the Lame constants are satisfied, i.e., $\mu > 0,\ \lambda + 2\mu > 0$. The set D will be referred to as the scatterer and the complement of D is the exterior domain denoted by $D_e = \mathbb{R}^2 \setminus \overline{D}$.

In what follows we assume time-spectral decomposition $\mathbf{U}(\mathbf{r},\, t) = \mathbf{u}(\mathbf{r})\, e^{-i\omega\, t}$. Therefore the governing equation of linearized elasticity that the displacement field satisfies is the well known spectral Navier equation

$$c_s^2\, \Delta \mathbf{u}(\mathbf{r}) + (c_p^2 - c_s^2) \nabla \nabla \cdot \mathbf{u}(\mathbf{r}) + \omega^2\, \mathbf{u}(\mathbf{r}) = \mathbf{0} \tag{1}$$

with ω being the angular frequency (denotes the Fourier dual variable of t), and c_p, c_s are the phase velocities of the longitudinal and the transverse wave, respectively, given by

$$c_p = \sqrt{\frac{\lambda + 2\mu}{\rho}}, \qquad c_s = \sqrt{\frac{\mu}{\rho}}$$

In addition, the above phase velocities are connected with ω via the relations $\omega = k_p c_p = k_s c_s$, where $k_p = 2\pi/\lambda_p$ and $k_s = 2\pi/\lambda_s$ are the wave numbers for the longitudinal and the transverse waves, respectively, and λ_p, λ_s are the corresponding wavelengths.

The well-known Helmholtz decomposition for the displacement field holds and is expressed via the relation $\mathbf{u}(\mathbf{r}) = \mathbf{u}^p(\mathbf{r}) + \mathbf{u}^s(\mathbf{r})$, where $\mathbf{u}^p(\mathbf{r})$ is the longitudinal part (P-wave), whereas $\mathbf{u}^s(\mathbf{r})$ the transverse part (S-wave). An abbreviation form of the differential equation (1) for which the displacement field satisfies in the exterior domain D_e is given by

$$(\Delta^* + \rho\,\omega^2)\mathbf{u}(\mathbf{r}) = \mathbf{0} \tag{2}$$

where the linear differential operator Δ^* is defined as

$$\Delta^* = \mu\Delta + (\lambda + \mu)\,\nabla\nabla\cdot\,. \tag{3}$$

We also define the surface stress operator (traction) on ∂D

$$T^{(\mathbf{r})} = 2\mu\,\hat{\mathbf{n}}_\mathbf{r}\cdot\nabla + \lambda\,\hat{\mathbf{n}}_\mathbf{r}\nabla\cdot + \mu\,\hat{\mathbf{n}}_\mathbf{r}\times\nabla\times, \tag{4}$$

where $\hat{\mathbf{n}}_r$ is the outward unit normal vector on the C^2- boundary ∂D at the point $\mathbf{r}$, and as usual the " $\cdot$ " denotes the scalar product, whereas the " $\times$ " denotes the vector one. The superscript in relation (4) denotes the action of the differential operator on the indicated variable (will be omitted from now on).

We now proceed with the scattering process, considering that our scatterer is irradiated by an elastic plane wave of the form

$$\mathbf{u}^{inc}(\mathbf{r}) = \hat{\mathbf{d}}\,e^{ik_p\mathbf{r}\cdot\hat{d}} + \hat{\mathbf{d}}^\perp\,e^{ik_s\mathbf{r}\cdot\hat{d}}, \tag{5}$$

where $\hat{\mathbf{d}}$ is the direction of propagation and $\hat{\mathbf{d}^\perp}$ the polarization vector with $\hat{\mathbf{d}} \in \Omega := \{\mathbf{r} \in \mathbb{R}^2 : |\,\hat{\mathbf{d}}\,| = 1\}$.

Due to the plane wave incident field (5), the disturbance for the scatterer D is expressed by the generation of a scattered field, denoted by $\mathbf{u}^{sct}$. Then the total field in the exterior domain D_e is denoted by $\mathbf{u}^{tot}$, expressed as the superposition of the incident field and the scattered wave, i.e.,

$$\mathbf{u}^{tot}(\mathbf{r}) = \mathbf{u}^{inc}(\mathbf{r}) + \mathbf{u}^{sct}(\mathbf{r}), \quad \mathbf{r} \in D_e \tag{6}$$

where the incident, the scattered and the total field satisfy Eq. (1). In addition the scattered field $\mathbf{u}^{sct}$ due to the Helmholtz decomposition is written as $\mathbf{u}^{sct}(\mathbf{r}) = \mathbf{u}^{sct,p}(\mathbf{r}) + \mathbf{u}^{sct,s}(\mathbf{r})$, where the vector functions $\mathbf{u}^{sct,p}$ and $\mathbf{u}^{sct,s}$ are the longitudinal (pressure) and transverse (shear) parts of $\mathbf{u}^{sct}$, respectively. The latter functions, satisfy the vector Helmholtz equations

$$(\Delta + k_p^2)\mathbf{u}^{sct,p}(\mathbf{r}) = \mathbf{0}, \quad (\Delta + k_s^2)\mathbf{u}^{sct,s}(\mathbf{r}) = \mathbf{0} \quad \mathbf{r} \in D_e \tag{7}$$

with $\mathbf{u}^{sct,p}$ and $\mathbf{u}^{sct,s}$ being rotational and divergence-free, respectively.

From the mathematical point of view, we consider a direct scattering problem which is described by the following boundary value problem:

(BVP1): *For a given scatterer $D \subset \mathbb{R}^2$ and an incident plane wave $\mathbf{u}^{inc}$, find a solution $\mathbf{u}^{sct} \in \left[C^2(D_e)\right]^2 \cap \left[C^1(D_e)\right]^2$, such that*

$$\Delta^* \mathbf{u}^{sct}(\mathbf{r}) + \rho\,\omega^2 \mathbf{u}^{sct}(\mathbf{r}) = \mathbf{0}, \quad \mathbf{r} \in D_e \tag{8}$$

$$\mathbf{u}^{sct}(\mathbf{r}) = \mathbf{0}, \quad \mathbf{r} \in \partial D \tag{9}$$

$$\lim_{r\to\infty} \sqrt{r}\left(\frac{\partial \mathbf{u}^{sct}_{(\beta)}(\mathbf{r})}{\partial r} - ik_\beta\, \mathbf{u}^{sct}_{(\beta)}(\mathbf{r})\right) = 0, \quad \beta = p, s, \quad r := |\mathbf{r}| \tag{10}$$

Relations (10) are the so-called Kupradze radiation conditions [14], for the P and S-components of the scattered field $\mathbf{u}^{sct,p}$, $\mathbf{u}^{sct,s}$, respectively, which hold uniformly over all directions $\hat{\mathbf{r}} = \mathbf{r}/r$.

Remark. The solvability of the above direct scattering problem (8)-(10) can be treated with analogous arguments (boundary integral equation approach) as those used in [16]. Uniqueness, existence for solutions as well as regularity results, can be proved for both smooth and Lipschitz boundaries. Since our aim in the work at hand is the study of the corresponding inverse elastic problem, we do not present these solvability results for the sake of brevity.

In what follows, we present the free-space Green's dyadic of the Navier equation (1), $\widetilde{\Gamma}(\mathbf{r},\, \mathbf{r}')$, given by

$$\begin{aligned}\widetilde{\Gamma}(\mathbf{r},\, \mathbf{r}') \;=\; & \frac{i}{4}\{\frac{1}{\mu}\widetilde{I} H_0^{(1)}(k_s|\mathbf{r}-\mathbf{r}'|) \\ & -\frac{1}{\rho\omega^2}\nabla_{\mathbf{r}} \otimes \nabla_{\mathbf{r}}\left[H_0^{(1)}(k_p|\mathbf{r}-\mathbf{r}'|) - H_0^{(1)}(k_s|\mathbf{r}-\mathbf{r}'|)\right]\}\end{aligned} \tag{11}$$

which satisfies the following equation

$$\Delta^* \widetilde{\Gamma}(\mathbf{r},\, \mathbf{r}') + \rho\,\omega^2 \widetilde{\Gamma}(\mathbf{r},\, \mathbf{r}') = -\widetilde{I}\,\delta(\mathbf{r}-\mathbf{r}'), \quad \mathbf{r},\, \mathbf{r}' \in \mathbb{R}^2 \tag{12}$$

with $\delta(\mathbf{r}-\mathbf{r}')$ being the Dirac measure concentrated at the point $\mathbf{r}$. Exploiting Betti's formulae, an integral representation for the radiating solution $\mathbf{u}^{sct} \in [C^2(D_e)]^2 \cap [C^1(D_e]^2$ of the Navier equation is given by

$$\mathbf{u}^{sct}(\mathbf{r}) = \int_{\partial D}\left[\left(T^{\mathbf{r}'}\widetilde{\Gamma}(\mathbf{r},\, \mathbf{r}')\right)^{\top} \cdot \mathbf{u}^{sct}(\mathbf{r}') - \widetilde{\Gamma}(\mathbf{r},\, \mathbf{r}') \cdot T^{\mathbf{r}'}\mathbf{u}^{sct}(\mathbf{r}')\right] ds(\mathbf{r}'), \tag{13}$$

where $\mathbf{r} \in D_e$, "$\top$" denotes transposition, and the superscript denotes the action of the differential operator on the indicated variable. From (13) and using asymptotic analysis, any radiating solution has the asymptotic behavior of the form

$$\mathbf{u}^{sct}(\mathbf{r}) = \mathbf{u}^{\infty,p}(\hat{\mathbf{r}})\frac{e^{ik_p r}}{\sqrt{r}} + \mathbf{u}^{\infty,s}(\hat{\mathbf{r}})\frac{e^{ik_s r}}{\sqrt{r}} + O(r^{-3/2}), \;\; r = |\mathbf{r}| \to \infty, \tag{14}$$

uniformly with respect to $\hat{\mathbf{r}} = \frac{\mathbf{r}}{r} \in \Omega$. The functions $\mathbf{u}^{\infty,p}$ and $\mathbf{u}^{\infty,s}$ are the corresponding far-field patterns, defined on the unit circle Ω in $\mathbb{R}^2$, where $\mathbf{u}^{\infty,p}(\hat{\mathbf{r}})$

is normal to Ω and $\mathbf{u}^{\infty,s}(\hat{\mathbf{r}})$ is tangential to Ω, and are known as the $P-$part (longitudinal) and the $S-$part (transverse) of the far-field pattern of $\mathbf{u}^{sct}$.

3. The Factorization Method.

For convenience in dealing with the numerical formulation, we would like to avoid the dyadic nature of the problem and hence we convert our equations in vector form. To this end, if $\mathbf{p} \in \Omega$ denotes the polarization of an elastic point-source at any $\mathbf{y}_0 \in \mathbb{R}^2$, then $\widetilde{\Gamma}(\mathbf{r},\, \mathbf{y}_0) \cdot \mathbf{p} \equiv \Gamma(\mathbf{r},\, \mathbf{y}_0; \mathbf{p}),\ \mathbf{r} \in \mathbb{R}^2 \setminus \{\mathbf{y}_0\}$. Using asymptotic analysis, $\Gamma(\mathbf{r},\, \mathbf{y}_0; \mathbf{p})$ can take the form

$$\begin{aligned} \Gamma(\mathbf{r},\, \mathbf{y}_0; \mathbf{p}) &= \Gamma^{\infty,p}(\mathbf{r},\, \mathbf{y}_0; \mathbf{p}) \frac{e^{ik_p r}}{\sqrt{r}} \hat{\mathbf{r}} \\ &\quad + \Gamma^{\infty,s}(\mathbf{r},\, \mathbf{y}_0; \mathbf{p})\ \frac{e^{ik_s r}}{\sqrt{r}} \hat{\mathbf{r}}^{\perp} + O(r^{-3/2}),\ \ r \to \infty \end{aligned} \tag{15}$$

with $\hat{\mathbf{r}}^{\perp}$ being the perpendicular vector to $\hat{\mathbf{r}}$. Hence

$$\Gamma^{\infty}(\mathbf{r},\, \mathbf{y}_0; \mathbf{p}) = \Gamma^{\infty,p}(\hat{\mathbf{r}},\, \mathbf{y}_0; \mathbf{p})\mathbf{r} + \Gamma^{\infty,s}(\hat{\mathbf{r}},\, \mathbf{y}_0; \mathbf{p})\hat{\mathbf{r}} \tag{16}$$

where the P $(\Gamma^{\infty,p}(\cdot,\, \mathbf{y}_0; \mathbf{p}))$ and S-part $(\Gamma^{\infty,s}(\cdot,\, \mathbf{y}_0; \mathbf{p}))$ of $\Gamma^{\infty}(\mathbf{r},\, \mathbf{y}_0; \mathbf{p})$ are given by

$$\Gamma^{\infty,p}(\hat{\mathbf{r}},\, \mathbf{y}_0; \mathbf{p}) = \frac{1}{\lambda + 2\mu}\, \frac{i+1}{4\sqrt{\pi k_p}}\ e^{-ik_p \hat{\mathbf{r}} \cdot \mathbf{y}_0}\ \hat{\mathbf{r}} \cdot \mathbf{p}, \tag{17}$$

$$\Gamma^{\infty,s}(\hat{\mathbf{r}},\, \mathbf{y}_0; \mathbf{p}) = \frac{1}{\mu}\, \frac{i+1}{4\sqrt{\pi k_s}}\ e^{-ik_s \hat{\mathbf{r}} \cdot \mathbf{y}_0}\ \hat{\mathbf{r}}^{\perp} \cdot \mathbf{p}, \tag{18}$$

respectively. Given that the far-field pattern $\mathbf{u}^{\infty}$ is defined as

$$\mathbf{u}^{\infty} = \mathbf{u}^{\infty,p}(\hat{\mathbf{r}})\hat{\mathbf{r}} + \mathbf{u}^{\infty,s}(\hat{\mathbf{r}})\hat{\mathbf{r}}^{\perp} \tag{19}$$

we can rewrite equation (14) in a more convenient form by noting that $\mathbf{u}^{\infty,p}(\hat{\mathbf{r}}) = \mathbf{u}^{\infty}(\hat{\mathbf{r}}) \cdot \hat{\mathbf{r}}$ and $\mathbf{u}^{\infty,s}(\hat{\mathbf{r}}) = \mathbf{u}^{\infty}(\hat{\mathbf{r}}) \cdot \hat{\mathbf{r}}^{\perp}$ as

$$\mathbf{u}^{sct}(\mathbf{r}) = \mathbf{u}^{\infty,p}(\hat{\mathbf{r}}) + \mathbf{u}^{\infty,s}(\hat{\mathbf{r}})\hat{\mathbf{r}}^{\perp} \tag{20}$$

where $\mathbf{u}^{\infty,p}(\hat{\mathbf{r}})$ and $\mathbf{u}^{\infty,s}(\hat{\mathbf{r}})$ are computed via parametrization as in [11] after we make the ansatz for the scattered field $\mathbf{u^{sc}}$ in the form

$$\mathbf{u}^{sc}(\mathbf{r}) = \int_{\partial\Omega} \Gamma(\mathbf{r}, \mathbf{r}')\phi(\mathbf{r}')ds(\mathbf{r}'),\ \mathbf{r} \in \mathbb{R}^3 \backslash \bar{\Omega}$$

with some function $\phi(\mathbf{r}) \in L^2(\partial\Omega)^2$.

We are now ready to formulate the $(F^{\star}F)^{1/4}$-method involving full far-field patterns which we will use for the reconstruction of the boundary ∂D of the rigid scatterer D.

We begin by introducing the incident field

$$v_g^{inc}(\mathbf{r}) = e^{-\frac{i\pi}{4}} \int_{\Omega} \left[\sqrt{\frac{k_p}{\omega}}\ \mathbf{g}_p(\hat{\mathbf{d}})\, e^{ik_p \mathbf{r} \cdot \hat{\mathbf{d}}} + \sqrt{\frac{k_s}{\omega}}\ \mathbf{g}_s(\hat{\mathbf{d}})\, e^{ik_s \mathbf{r} \cdot \hat{\mathbf{d}}} \right] ds(\hat{\mathbf{d}}) \tag{21}$$

The above relation refers to a superposition of plane waves over the unit circle Ω propagating in every direction. The density function $\mathbf{g} \in [L^2(\Omega)]^2$ and its components $\mathbf{g}_p$, $\mathbf{g}_s$ are known as the longitudinal and transverse Herglotz kernels given by

$$\mathbf{g}_p(\hat{\mathbf{d}}) = g_p(d)\,\hat{\mathbf{d}}, \qquad \mathbf{g}_s(\hat{\mathbf{d}}) = g_s(d)\,\hat{\mathbf{d}}^{\perp} \tag{22}$$

The far-field patterns of the scattered fields corresponding to the incident wave v_g^{inc} (see (21)), are expressed via the far-field operator $F : [L^2(\Omega)]^2 \to [L^2(\Omega)]^2$ given by

$$\begin{aligned}(F\mathbf{g})(\hat{\mathbf{r}}) &= e^{-\frac{i\pi}{4}} \Big[\int_\Omega \sqrt{\frac{k_p}{\omega}}\ \mathbf{u}^\infty(\hat{\mathbf{r}}, \hat{\mathbf{d}}, \hat{\mathbf{d}})\, g_p(d)\, ds(\hat{\mathbf{d}}) \\ &\quad + \int_\Omega \sqrt{\frac{k_s}{\omega}}\ \mathbf{u}^\infty(\hat{\mathbf{r}}, \hat{\mathbf{d}}, \hat{\mathbf{d}}^{\perp})\, g_s(d)\, ds(\hat{\mathbf{d}})\Big]\end{aligned} \tag{23}$$

where $e^{-\frac{i\pi}{4}} \sqrt{\frac{k_\alpha}{\omega}}\, g_\alpha$, $\alpha = p, s$ are the $L^2(\Omega)$-kernels, and $\hat{\mathbf{r}}, \hat{\mathbf{d}}$ denote the observation and incident directions, respectively. Hence $F\mathbf{g}$ is the far-field pattern for the scattering of the elastic Herglotz wavefunction with kernel $\mathbf{g}$.

For the far-field pattern $\mathbf{u}^\infty$, we introduce the following notation

$$\begin{aligned}\mathbf{u}^\infty(\cdot, \hat{\mathbf{d}}, \hat{\mathbf{d}}) &= (u^{\infty,p}(\cdot, \hat{\mathbf{d}}, \hat{\mathbf{d}}),\, u^{\infty,s}(\cdot, \hat{\mathbf{d}}, \hat{\mathbf{d}})) \\ \mathbf{u}^\infty(\cdot, \hat{\mathbf{d}}, \hat{\mathbf{d}}^{\perp}) &= (u^{\infty,p}(\cdot, \hat{\mathbf{d}}, \hat{\mathbf{d}}^{\perp}),\, u^{\infty,s}(\cdot, \hat{\mathbf{d}}, \hat{\mathbf{d}}^{\perp}))\end{aligned} \tag{24}$$

It is now apparent that the factorization method is employed to seek a density $\mathbf{g}(., \mathbf{z}, \mathbf{p})$, $\mathbf{z} \in D$, such that

$$(F^\star F)^{1/4} \mathbf{g}(., \mathbf{z}; \mathbf{p}) = \Gamma^\infty(., \mathbf{z}; \mathbf{p}) \tag{25}$$

4. Numerical Results

For N pressure waves or N shear waves, incident from N directions $d_j = (cos\theta_j, \sin\theta_j)$ with $\theta_j = (2\pi j/N)$, we assume that the far-field equation (25) is discretized as described in [11], giving rise to a system of $2N \times 2N$ linear equations

$$F^D g_{\mathbf{z}} = b^{(\mathbf{z})}, \quad F^D \in C^{2N \times 2N}, \tag{26}$$

where $b^{(\mathbf{z})}$ is a discrete version of $\mathbf{\Gamma}^\infty$ and F^D is a discretized version of the far-field operator $(F^\star F)^{1/4}$. We shall consider the reconstruction problem in three cases: a) FF case based on the operator F^D (full far-field pattern), b) PP case based on the operator F_p^D (part of the far-field pattern corresponding to N incident plane pressure waves), and c) SS case based on the operator F_s^D (part of the far-field pattern corresponding to N incident plane shear waves). A discretized version of F_p^D (resp. F_s^D) can be extracted from F^D by taking rows 1 (resp. $N+1$) through N (resp. $2N$) and columns 1 (resp. $N+1$) through N (resp. $2N$) [11]. In all cases, for some chosen polarization vector and for each

sampling point $\mathbf{z} \in \mathbb{R}^2$, the profile of the object can be recovered by plotting the indicator function

$$W = \left[\sum_{j=1}^{M} \frac{|\alpha_j^{(\mathbf{z})}|^2}{\eta_j} \right]^{-1} \tag{27}$$

where $M = 2N$ in the FF case or $M = N$ in the other cases, α_j is the component of $b^{(\mathbf{z})}$ along the jth right singular vector of F in the FF case, or the component of $b^{(\mathbf{z},p)}$ (resp. $b^{(\mathbf{z},s)}$) along the jth right singular vector of F_p in the other case (resp. F_s), and η_j is the corresponding singular value. Here, $b^{(\mathbf{z},p)}$ (resp. $b^{(\mathbf{z},s)}$) denotes the vector of N first (resp. last) components of $b^{(\mathbf{z})}$.

Reconstructions obtained via the factorization method are based on fact that the values of W should be much smaller for $\mathbf{z} \notin D$ than for those lying within D.

We begin the discussion of our approach by considering the norm of the unregularized version of the solution i.e.

$$\|g\|_{L^2}^2 = \sum_{j=1}^{M} \frac{|\alpha_j^{(\mathbf{z})}|^2}{\eta_j}. \tag{28}$$

Our idea stems from the Picard condition [9]:

The exact SVD coefficients $|\alpha_j^{(\mathbf{z})}|$ decay faster than the μ_j's

as this will ensure that the solution for the ill-posed problem exists. More detailed discussion about the effects of Picard's condition in elastic scattering can be found in [15].

Consequently we define

$$V_i = \frac{1}{\sum_{j=1}^{i} \frac{|\alpha_j^{(\mathbf{z})}|^2}{\eta_j}} \tag{29}$$

with $i = 1, 2, \cdots M$.

Our approach is based on the fact that if the ratios

$$\frac{V_i}{V_1}, \;\; i = 1, 2, \cdots M \tag{30}$$

reach a certain tolerance, then a successful reconstruction will be achieved due to the removal of small singular values. The problem here though is that if our tolerance is very small we might include more eigenvalues than we need (and in some cases all of them) with catastrophic consequences to the quality of the reconstruction.

We hence begin by imposing a moderate tolerance of ϵ_1 to (30) which we will later adjust accordingly, i.e.

$$\frac{V_i}{V_1} < \epsilon_1, \;\; i = 1, 2, \cdots M \tag{31}$$

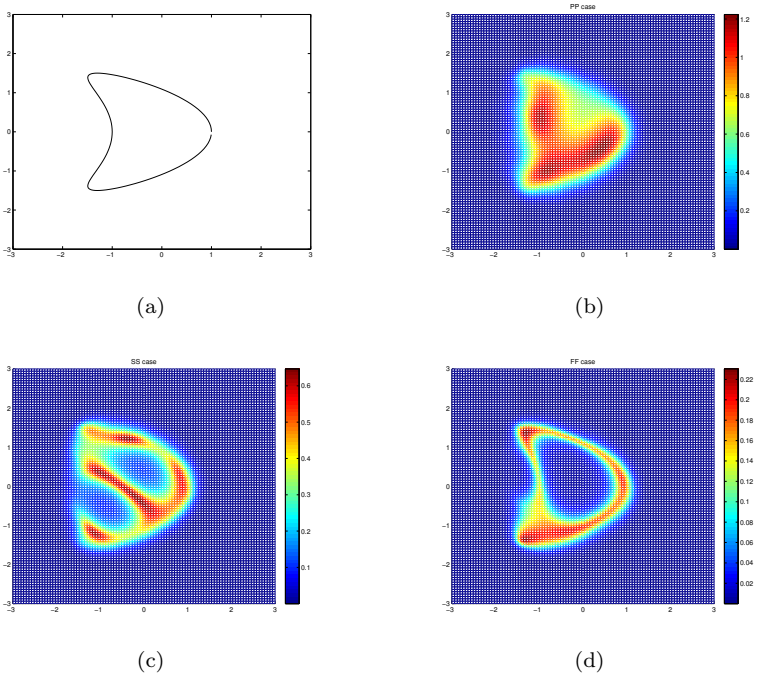

(a) (b)

(c) (d)

FIGURE 1. Exact profile of a kite (a), reconstruction of PP case (b). reconstruction of SS case(c), reconstruction of FF case (d).

In order to efficiently adjust the tolerance in (31) we introduce the following quantity

$$k_i = \frac{\eta_1}{\eta_i}, \quad i = 1, 2, \cdots M \tag{32}$$

which represents the condition number of the matrix A, that results from the discretized form of the far field operator F.

As soon as equation (31) reaches ϵ_1 we check the corresponding k_i. If it exceeds ϵ_2 we stop, otherwise we reduce ϵ_1 by half. The above process continuous till ϵ_2 is reached.

This algorithm is presented in ALGORITHM 4.1, and the variable nsv indicates the number of singular values used for the image reconstruction. Moreover we need to mention that the variable nsv is determined only once by using the $\mathbf{z}$ that corresponds to discretization position (1,1). Consequently, this nsv is used for all $\mathbf{z}$'s in the grid to yield the image reconstruction. The authors noticed that using all $\mathbf{z}$'s to determine nsv did not change its original value and the computational effort was significantly higher.

Algorithm 4.1. Regularization ratios

$nsv \leftarrow M$
for $i = 1, 2, \cdots, M$
  compute V_i
  if $V_i/V_1 < \epsilon_1$
    if $\eta_1/\eta_i < \epsilon_2$
      $\epsilon_1 \leftarrow \epsilon_1/2$
    else
      $nsv \leftarrow i$
      Break
    endif
  endif
endfor

For the numerical reconstructions we consider a uniform grid in the square $[2, 2] \times [2, 2]$ containing the object, with 100 points in each direction, and use noisy far-field matrices of order 64×64. The noise is introduced in the data via

$$\widetilde{F}^D = F^D + \epsilon \|F\| N, \tag{33}$$

where N is a random noise matrix normalized such that $\|N| = 1$ and ϵ is an error parameter which determines the amount of noise in the data. In our numerical experiments we have chosen $\epsilon = 0.1$ (relative noise level 1%). The reconstructions of a kite are shown in Figure 1 and illustrate the excellent performance of the method of regularized ratios which doesn't require (a)a-priori knowledge of the noise level in the data and (b) the solution of discrepancy equations at every point in the grid. Moreover, our reconstructions used approximately 35 singular values out of 64. This makes our method attractive for three dimensional reconstructions which is work in progress. It is important to point out here that ϵ_1 establishes the basic information to start the image reconstruction, whereas ϵ_2 enforces an efficient number of eigenvalues to be used to fine tune the image. In our numerical experiments we set $\epsilon_1 = 10^{-7}$ and $\epsilon_2 = 5 \times 10^2$. By looking at Figure 1 it becomes obvious that the FF case produced better reconstructions. We believe that this is due to the stronger singularities of the P-part and S-part of the scattered field as $\mathbf{z}$ approaches the boundary from outside. For more details we refer the reader to [11].

References

[1] C.J.S Alves and R. Kress, 2002 On the far field operator in elastic obstacle scattering *IMA J. Appl. Math.* **67** 1–21

[2] K. Anagnostopoulos and A. Charalambopoulos. The linear sampling method for the transmission problem in 2D anisotropic elasticity *Inverse Problems* (2006) **22**, 553-577.

[3] F. Cakoni and D. Colton *Qualitative Methods in Inverse Scattering Theory: An Introduction.*(Springer-Verlag), 1988.

[4] D. Colton *Partial Differential Equations: An Introduction.* (New York:Random House, Inc.), 1988.
[5] D. Colton and R. Kress, *Inverse Acoustic and Electromagnetic Scattering Theory.* (New York:Springer-Verlag), 1992.
[6] D. Colton and A. Kirsch, A simple method for solving the inverse scattering problems in the resonance region. *Inverse Problems* (1996) **12**, 383-393.
[7] D. Colton, M. Piana and R. Potthast, A simple method using Morozov's discrepancy principle for solving inverse scattering problems, *Inverse Problems* (1999) **13**, 1477-93
[8] D. Natrosvilli, Z. Tediashvili, *Mixed type direct and inverse scattering problems*, in *Problems and Methods in Mathematical Physics* (eds. Elschner J, Gohberg I and Silbermann B), *Operator Theory: Advances and Applications*(2001) **121** (Birkhäuser, Basel) 366–389
[9] P. C. Hansen *Rank-Deficient and Descrete Ill-Posed Problems.* SIAM, Philadelphia, 1998.
[10] P. C. Hansen *The L-Curve and its use in the numerical treatment of inverse problems.* Computational Inverse Problems in Electrocardiology. *WIT Press* 119-142 (2001)
[11] G. Hu, A. Kirsch and M. Sini, *Some Inverse Problem arising from elastic scattering by rigid obstacles*, Inverse Problems (2013) **29**, 1-21
[12] A. Kirsch, Characterization of the shape of a scattering obstacle using the spectral data of the far field operator. *Inverse Problems* (1998) **14**, 1489-1512.
[13] K.Kim, K.H. Leem and G. Pelekanos *An Alternative to Tikhonov Regularization for Linear Sampling Methods*, Acta Applicandae Mathematicae (2010) **112**, 171-180.
[14] V. D. Kupradze, *Dynamical Problems in Elasticity, in "Progress in Solid Mechanics".* North-Holland, Amsterdam (1963).
[15] G. Pelekanos and V. Sevroglou, Shape reconstrution of a 2D-elastic penetrable object via the L-curve method. *J. Inv. Ill-Posed problems* (2006) **14**, No.4, 1-16.
[16] Pelekanos G and Sevroglou V 2003 Inverse scattering by penetrable objects in two-dimensional elastodynamics *J. Comp. Appl. Math.* **151** 129–140
[17] Sevroglou V and Pelekanos G 2001 An inversion algorithm in two-dimensional elasticity *J. Math. Anal. Appl.* **263** 277–293
[18] Sevroglou V and Pelekanos G 2002 Two dimensional elastic Herglotz functions and their applications in inverse scattering *Journal of Elasticity* **68** 123–144
[19] Sevroglou V 2005 The far–field operator for penetrable and absorbing obstacles in 2D inverse elastic scattering *Inverse Problems* **17** 717–738

K.Kim
Department of Mathematics, Yeungnam University, 719-749, Gyeongsangbuk-do, South Korea
E-mail address: khkim@ynu.ac.kr

K.H.Leem
Department of Mathematics and Statistics, Southern Illinois University, Edwardsville, IL 62026, USA
E-mail address: kleem@siue.edu

G. Pelekanos
Department of Mathematics and Statistics, Southern Illinois University, Edwardsville, IL 62026, USA
E-mail address: gpeleka@siue.edu